Adaptive Control for Teleoperation System With Varying Time Delays and Input Saturation Constraints

Di-Hua Zhai and Yuanqing Xia, *Senior Member, IEEE*

***Abstract*—This paper addresses the adaptive control of teleoperation system with actuator saturation. To unify the study of actuator saturation, passive/nonpassive external forces, asymmetric time-varying delays, and unknown dynamics in the same framework, a novel switched control scheme is developed, where a special switched filter is investigated. In the saturation scenario, the designed controller consists of a generalized controller and a nonlinear saturation function. By placing the nonlinear saturation function on the outside of the generalized controller, and further jointing with the design of switched filter, the designed generalized controller needs not consider the actuator saturation. Specifically, it is designed to be in the form of proportional plus damping injection plus switched filter. Then, the complete closed-loop system is modeled as a special switched system. It is finally established to be state-independent input-to-output stable, where the ultimate boundedness of the tracking error is ensured for any bounded exogenous forces, which is demonstrated by the experimental studies.**

***Index Terms*—Actuator saturation, adaptive control, asymmetric time-varying delay, state-independent input-to-output stable (SIIOS), switched control, teleoperation.**

I. Introduction

OVER the past decades, teleoperation system that enables a human operator to act as a remote robot at a distance by the exchange of various information has attracted a lot of attention [1]–[10]. Among them, one major concern is the nonzero communication delay, which is a formidable barrier to achieve a high level of fidelity while maintaining system stability. Several works offer a variety of Lyapunov–Krasovskii stability analysis, such as constant delay [11]–[14], time-varying delay [15]–[18], and random delay [19], just to name a few, where the passivity-based methodology is a prevalent one [20]. Recently, some interesting results for nonpassive human operator based teleoperation systems are also introduced in [21]–[25]. Since it does not require that human operator, master, slave, environment, and communication networks are passive, they are more likely to be satisfied in practices. Unfortunately, none of them consider the actuator saturation. In practices, the actuator inevitably possesses a limited output capacity, which may cause undesirable responses [26]–[28]. Therefore, the actuator saturation should be considered. For the robotic systems including teleoperation systems, several approaches have been reported. In [29], a nonlinear proportional plus gravity compensation controller design is developed for single robot, where the position error passes through a saturating function. An improved method with adaptive gravity compensation is also reported in [30]. Since they do not consider the communication delay, they cannot be applied to teleoperation system. Recently, the saturated control for teleoperation system with time delays are also developed, e.g., the constant delay case [31], [32] and the time-varying delay case [34]. In [34], a nonlinear proportional plus damping injection scheme is investigated, which unifies the study of actuator saturation and varying time delay in the same framework. However, those results are performed based on passive framework, which may face some difficulties in implementation in practices [21]. In addition, a further extension of [34] to adaptive scenario still faces many technique challenges. In this paper, a novel adaptive control is developed for teleoperation system with actuator saturation. First, in the saturation scenario, the designed controller consists of two parts: a generalized controller based on switching technique and a nonlinear saturating function. To simplify the design, the nonlinear saturating function is placed on the outside of the generalized controller. Thus, the design of the generalized controller needs not consider the saturation level of the actuator. Second, in the actuator saturation scenario, to make the most of the state information, based on the concept of dynamic compensation, an auxiliary generalized switched filter is developed, which is different from the previous work [33]. Then, the generalized controller is designed to be in the form of proportional plus damping injection plus generalized switched filter. Finally, the complete closed-loop master (slave) system is modeled as a special switched system. By using the multiple Lyapunov–Krasovskii functionals approach, the state-independent input-to-output stability (SIIOS) is established. The new framework unifies the study of the passive and nonpassive external forces, and therefore, it can reduce the conservativeness of conventional assumption as pointed out by Polushin *et al.* [21], [23].

Manuscript received December 13, 2015; revised March 31, 2016; accepted May 1, 2016. Date of publication June 21, 2016; date of current version October 7, 2016. This work was supported in part by the National Basic Research Program of China (973 Program) under Grant 2012CB720000, in part by the National Natural Science Foundation of China under Grant 61225015, Grant 61105092, and Grant 61422102, in part by the Beijing Natural Science Foundation under Grant 4161001, and in part by the Foundation for the Innovative Research Groups of the National Natural Science Foundation of China under Grant 61321002.
(Corresponding author: Yuanqing Xia.)

The authors are with the School of Automation, Beijing Institute of Technology, Beijing 100081 China (e-mails: zhaidih@gmail.com; xia_yuanqing@bit.edu.cn).

Color versions of one or more of the figures in this paper are available online at http://ieeexplore.ieee.org.

Digital Object Identifier 10.1109/TIE.2016.2583199

II. Problem Formulation

A. Dynamics of Teleoperated Robots

Let us consider the following teleoperation system:

$$\begin{cases} \boldsymbol{M}_m(\boldsymbol{q}_m)\ddot{\boldsymbol{q}}_m + \boldsymbol{C}_m(\boldsymbol{q}_m,\dot{\boldsymbol{q}}_m)\dot{\boldsymbol{q}}_m + \boldsymbol{g}_m(\boldsymbol{q}_m) \\ \qquad + \boldsymbol{f}_m(\dot{\boldsymbol{q}}_m) + \boldsymbol{d}_m = \boldsymbol{J}_m^T(\boldsymbol{q}_m)\boldsymbol{f}_h + \boldsymbol{\tau}_m \\ \boldsymbol{M}_s(\boldsymbol{q}_s)\ddot{\boldsymbol{q}}_s + \boldsymbol{C}_s(\boldsymbol{q}_s,\dot{\boldsymbol{q}}_s)\dot{\boldsymbol{q}}_s + \boldsymbol{g}_s(\boldsymbol{q}_s) \\ \qquad + \boldsymbol{f}_s(\dot{\boldsymbol{q}}_s) + \boldsymbol{d}_s = -\boldsymbol{J}_s^T(\boldsymbol{q}_s)\boldsymbol{f}_e + \boldsymbol{\tau}_s. \end{cases} \tag{1}$$

The end-effector positions $\boldsymbol{x}_m \in \mathbb{R}^n$ and $\boldsymbol{x}_s \in \mathbb{R}^n$ are

$$\boldsymbol{x}_j = \boldsymbol{h}_j(\boldsymbol{q}_j),\ \dot{\boldsymbol{x}}_j = \boldsymbol{J}_j(\boldsymbol{q}_j)\dot{\boldsymbol{q}}_j,\ j = m, s.$$

The environment and operator dynamics are modeled as [35]

$$\begin{cases} \boldsymbol{f}_h = \boldsymbol{f}_h^* - M_h\ddot{\boldsymbol{x}}_m - B_h\dot{\boldsymbol{x}}_m - K_h\boldsymbol{x}_m \\ \boldsymbol{f}_e = \boldsymbol{f}_e^* + M_e\ddot{\boldsymbol{x}}_s + B_e\dot{\boldsymbol{x}}_s + K_e\boldsymbol{x}_s. \end{cases} \tag{2}$$

It is also assumed that the human operator (the environment) exogenous force $\boldsymbol{f}_h^*$ ($\boldsymbol{f}_e^*$) is locally essentially bounded.

Remark 2.1: A function $\boldsymbol{\nu}$ is said to be essentially bounded if $ess\sup_{t\geq 0}|\boldsymbol{\nu}(t)| < \infty$. For any given $0 \leq a < b$, we indicate with $\boldsymbol{\nu}_{[a,b)} : [0,\infty) \to \mathbb{R}^m$ the function given by $\boldsymbol{\nu}_{[a,b)}(t) = \boldsymbol{\nu}(t)$ for all $t \in [a, b)$ and $= 0$ elsewhere. An input $\boldsymbol{\nu}$ is said to be locally essentially bounded if, for any $T > 0$, $\boldsymbol{\nu}_{[0,T)}$ is essentially bounded.

Substituting (2) into (1), it has

$$\begin{cases} \boldsymbol{\mathcal{M}}_m(\boldsymbol{q}_m)\ddot{\boldsymbol{q}}_m + \boldsymbol{\mathcal{C}}_m(\boldsymbol{q}_m,\dot{\boldsymbol{q}}_m)\dot{\boldsymbol{q}}_m + K_h\boldsymbol{h}_m(\boldsymbol{q}_m) \\ \quad + \boldsymbol{f}_m(\dot{\boldsymbol{q}}_m) + \boldsymbol{g}_m(\boldsymbol{q}_m) + \boldsymbol{d}_m = \boldsymbol{J}_m^T(\boldsymbol{q}_m)\boldsymbol{f}_h^* + \boldsymbol{\tau}_m \\ \boldsymbol{\mathcal{M}}_s(\boldsymbol{q}_s)\ddot{\boldsymbol{q}}_s + \boldsymbol{\mathcal{C}}_s(\boldsymbol{q}_s,\dot{\boldsymbol{q}}_s)\dot{\boldsymbol{q}}_s + K_e\boldsymbol{h}_s(\boldsymbol{q}_s) \\ \quad + \boldsymbol{f}_s(\dot{\boldsymbol{q}}_s) + \boldsymbol{g}_s(\boldsymbol{q}_s) + \boldsymbol{d}_s = -\boldsymbol{J}_s^T(\boldsymbol{q}_s)\boldsymbol{f}_e^* + \boldsymbol{\tau}_s \end{cases} \tag{3}$$

where for all $j = m, s$

$$\begin{aligned} \boldsymbol{\mathcal{M}}_j(\boldsymbol{q}_j) &= \boldsymbol{M}_j(\boldsymbol{q}_j) + \boldsymbol{J}_j^T(\boldsymbol{q}_j)M_{he_j}\boldsymbol{J}_j(\boldsymbol{q}_j) \\ \boldsymbol{\mathcal{C}}_j(\boldsymbol{q}_j,\dot{\boldsymbol{q}}_j) &= \boldsymbol{C}_j(\boldsymbol{q}_j,\dot{\boldsymbol{q}}_j) + \boldsymbol{J}_j^T(\boldsymbol{q}_j)B_{he_j}\boldsymbol{J}_j(\boldsymbol{q}_j) \\ &\quad + \boldsymbol{J}_j^T(\boldsymbol{q}_j)M_{he_j}\dot{\boldsymbol{J}}_j(\boldsymbol{q}_j) \end{aligned}$$

with $M_{he_m} = M_h$, $M_{he_s} = M_e$, $B_{he_m} = B_h$, $B_{he_s} = B_e$. System (3) satisfies the properties of robotic system [36].

Property 2.1: There exist $\rho_{j1}, \rho_{j2} > 0$ such that $\rho_{j1}\boldsymbol{I} \leq \boldsymbol{\mathcal{M}}_j(\boldsymbol{q}_j) \leq \rho_{j2}\boldsymbol{I}$, where $j = m, s$, $\boldsymbol{I}$ is identity matrix with appropriate dimensions.

Property 2.2: For any $\boldsymbol{x} \in \mathbb{R}^n$, $\boldsymbol{x}^T(\dot{\boldsymbol{M}}_j(\boldsymbol{q}_j) - 2\boldsymbol{C}_j(\boldsymbol{q}_j, \dot{\boldsymbol{q}}_j))\boldsymbol{x} = 0$, where $j = m, s$.

Remark 2.2: Since M_h, B_h (M_e, B_e) are constant scalars, one can further obtain $\boldsymbol{x}^T(\dot{\boldsymbol{\mathcal{M}}}_j(\boldsymbol{q}_j) - 2\boldsymbol{\mathcal{C}}_j(\boldsymbol{q}_j,\dot{\boldsymbol{q}}_j))\boldsymbol{x} = -2\boldsymbol{x}^T\boldsymbol{J}_j^T(\boldsymbol{q}_j)B_{he_j}\boldsymbol{J}_j(\boldsymbol{q}_j)\boldsymbol{x}$, where $B_{he_m} = B_h$, $B_{he_s} = B_e$.

For the existed unknown dynamics, it is assumed

Assumption 2.1: For all $j = m, s$, it is assumed: $|K_{he_j}h_j(\boldsymbol{q}_j)| \leq k_{j1}$, $|\boldsymbol{f}_j(\dot{\boldsymbol{q}}_j)| \leq k_{j2} + k_{j3}|\dot{\boldsymbol{q}}_j|$, $|\boldsymbol{g}_j(\boldsymbol{q}_j)| \leq k_{j4}$, $|\boldsymbol{d}_j| \leq k_{j5}$, $|\boldsymbol{J}_j^T(\boldsymbol{q}_j)\boldsymbol{J}_j(\boldsymbol{q}_j)\dot{\boldsymbol{q}}_j| \leq k_{j6}|\dot{\boldsymbol{q}}_j|$, where $K_{he_m} = K_h$, $K_{he_s} = K_e$, $k_{j1}, k_{j2}, \ldots, k_{j6}$ are unknown positive constants.

In Assumption 2.1, k_{j3} and k_{j6} are related to $|\dot{\boldsymbol{q}}_j|$, while others are not. In what follows, for simplicity, let $\omega_{j1} = k_{j1} + k_{j2} + k_{j4} + k_{j5}$ and $\omega_{j2} = k_{j3} + k_{j6}$. Then, only two adaptive estimators need be used to estimate ω_{j1} and ω_{j2}.

B. Actuator Model and the Nonlinear Saturation Function

In practices, the actuator inevitably possesses a limited output capacity. Therefore, let $\boldsymbol{\tau}_j = [\tau_{j1}, \tau_{j2}, \ldots, \tau_{jn}]^T$ as

$$\tau_{ji} = \begin{cases} \tau_{ji}, & |\tau_{ji}| \leq \tau_M \\ \tau_{Mi}\text{sgn}(\tau_{ji}), & |\tau_{ji}| > \tau_M \end{cases},\ i = 1, 2, \ldots, n$$

where τ_M is the upper bound of torque output of the joint actuators. To cope with the saturation in actuators, a nonlinear saturating function, $\boldsymbol{\mathcal{P}}(\cdot)$, is introduced, i.e.,

$$\boldsymbol{\tau}_j = \boldsymbol{\mathcal{P}}(\bar{\boldsymbol{\tau}}_j) = [\mathcal{P}_1(\bar{\tau}_{j1}), \mathcal{P}_2(\bar{\tau}_{j2}), \ldots, \mathcal{P}_n(\bar{\tau}_{jn})]^T \in \mathbb{R}^n \tag{4}$$

where $\bar{\boldsymbol{\tau}}_{\boldsymbol{j}} = [\bar{\tau}_{j1}, \ldots, \bar{\tau}_{jn}]^T$ is the generalized controller without considering actuator saturation, $\mathcal{P}_i(\bar{\tau}_{ji})$ is given by

$$\mathcal{P}_i(\bar{\tau}_{ji}) = \tau_M(1 - e^{-|\bar{\tau}_{ji}|})sgn(\bar{\tau}_{ji}),\ i = 1, 2, \ldots, n. \tag{5}$$

Obviously, $0 \leq |\mathcal{P}_i(\bar{\tau}_{ji})| \leq \tau_M$. Substituting $\boldsymbol{\tau}_j = \boldsymbol{\mathcal{P}}(\bar{\boldsymbol{\tau}}_j)$ into (3), it thus has

$$\begin{aligned} &\boldsymbol{\mathcal{M}}_j(\boldsymbol{q}_j)\ddot{\boldsymbol{q}}_j + \boldsymbol{\mathcal{C}}_j(\boldsymbol{q}_j,\dot{\boldsymbol{q}}_j)\dot{\boldsymbol{q}}_j + K_{he_j}\boldsymbol{h}_j(\boldsymbol{q}_j) + \boldsymbol{f}_j(\dot{\boldsymbol{q}}_j) \\ &\qquad + \boldsymbol{g}_j(\boldsymbol{q}_j) + \boldsymbol{d}_j = \boldsymbol{J}_j^T(\boldsymbol{q}_j)\boldsymbol{f}_{he_j} + \boldsymbol{\mathcal{P}}(\bar{\boldsymbol{\tau}}_j) \end{aligned} \tag{6}$$

where $\boldsymbol{f}_{he_m} = \boldsymbol{f}_h^*$, $\boldsymbol{f}_{he_s} = -\boldsymbol{f}_e^*$. To simplify the analysis, the nonlinear saturating function $\boldsymbol{\mathcal{P}}(\bar{\boldsymbol{\tau}}_j)$ will be rewritten as an affine nonlinear function with respect to $\bar{\boldsymbol{\tau}}_j$. According to the Lagrange mean value theorem, there exists $a \in [0, \bar{\tau}_{ji}]$ such that $\frac{e^{-\bar{\tau}_{ji}}-1}{\bar{\tau}_{ji}-0} = -e^{-a}$, i.e.,

$$1 - e^{-\bar{\tau}_{ji}} = e^{-a}\bar{\tau}_{ji},\ a \in [0, \bar{\tau}_{ji}],\ \bar{\tau}_{ji} > 0. \tag{7}$$

Similarly, it also has

$$1 - e^{\bar{\tau}_{ji}} = -e^{b}\bar{\tau}_{ji},\ b \in [\bar{\tau}_{ji}, 0],\ \bar{\tau}_{ji} < 0. \tag{8}$$

Equations (7) and (8) still hold when $\bar{\tau}_{ji} = 0$ with $a = b = 0$. Jointing (7) and (8) with (5), there exists $c_{ji} \in [0, |\bar{\tau}_{ji}|]$ such that

$$\mathcal{P}_i(\bar{\tau}_{ji}) = \tau_M e^{-c_{ji}}\bar{\tau}_{ji} \tag{9}$$

with $e^{-|\bar{\tau}_{ji}|} \leq e^{-c_{ji}} \leq 1$. And further, it has the affine system

$$\boldsymbol{\mathcal{P}}(\bar{\boldsymbol{\tau}}_j) = \tau_M\boldsymbol{\Xi}_j\bar{\boldsymbol{\tau}}_j$$

where $\boldsymbol{\Xi}_j = \text{diag}[e^{-c_{j1}}, e^{-c_{j2}}, \ldots, e^{-c_{jn}}] \in \mathbb{R}^{n\times n}$.

C. Control Objectives

For all $j = m, s$, the tracking errors are defined as

$$\begin{cases} \boldsymbol{e}_j(t) = \boldsymbol{q}_j(t) - \boldsymbol{q}_\ell(t - T_\ell(t)) \\ \boldsymbol{e}_{vj}(t) = \dot{\boldsymbol{q}}_j(t) - \dot{\boldsymbol{q}}_\ell(t - T_\ell(t)) \end{cases},\ \ell = m, s,\ \ell \neq j. \tag{10}$$

The control objective is to achieve the position synchronization between the master and slave robots. In what follows, it is assumed $0 \leq T_j(t) \leq \bar{T}$ and $0 \leq |\dot{T}_j(t)| \leq \tilde{T}$, where $\bar{T}$ and $\tilde{T}$ are positive constants.

Remark 2.3: This kind of bounded assumption does not affect the theoretic analysis, while some similar works can be seen in [24] and [9] and the references therein. However, in practices, $|\dot{T}_j(t)| \geq 1$ means that the delay grows faster than time, which may cause the control loop become open. To avoid the case, similar to [17], [24], [39], [40], the artificial communication

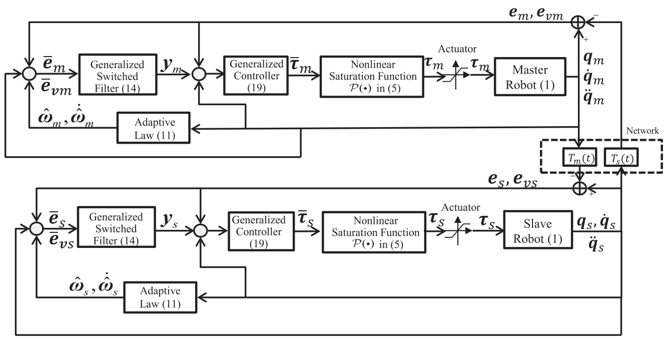

Fig. 1. Block diagram of the proposed control algorithm.

delays will be assumed to have $\tilde{T} < 1$ in the practical experiment in Section V. Finally, given that the rate of change of time delay may still be larger than or equal one, some other control techniques, for example, networked predictive controller [41], can be used to handle this more realistic scenario, which will be one of our future works.

III. Controller Design Based on Switching Control Technique

To perform the adaptive control for system (6) with actuator saturation, a novel switching control framework is developed, where Fig. 1 gives the block diagram. First, let $\hat{\omega}_{j1}(t)$ and $\hat{\omega}_{j2}(t)$ denote respectively the estimations of ω_{j1} and ω_{j2}. The update laws are given as

$$\begin{cases} \dot{\hat{\omega}}_{j1}(t) = -\psi_{j11}\hat{\omega}_{j1}(t) + \psi_{j12}P_{j1}\varepsilon_{j1}|\dot{\boldsymbol{q}}_j(t)|^2 \\ \dot{\hat{\omega}}_{j2}(t) = -\psi_{j21}\hat{\omega}_{j2}(t) + \psi_{j22}P_{j1}|\dot{\boldsymbol{q}}_j(t)|^2 \end{cases} \tag{11}$$

where P_{j1}, ψ_{ji1}, ψ_{ji2} $(i = 1, 2)$, and ε_{j1} are some positive constant scalars. Also, define the estimation errors $\tilde{\omega}_{j1}(t) = \omega_{j1} - \hat{\omega}_{j1}(t)$ and $\tilde{\omega}_{j2}(t) = \omega_{j2} - \hat{\omega}_{j2}(t)$.

Remark 3.1: By solving (11), one can obtain

$$\hat{\omega}_{j1}(t) = e^{-\psi_{j11}t}\hat{\omega}_{j1}(0) + \int_0^t e^{\psi_{j11}(w-t)}\psi_{j12}P_{j1}\varepsilon_{j1}|\dot{\boldsymbol{q}}_j(w)|^2 \mathrm{d}w$$

$$\hat{\omega}_{j2}(t) = e^{-\psi_{j21}t}\hat{\omega}_{j2}(0) + \int_0^t e^{\psi_{j21}(w-t)}\psi_{j22}P_{j1}|\dot{\boldsymbol{q}}_j(w)|^2 \mathrm{d}w.$$

For any $\hat{\omega}_{j1}(0) > 0$ $(\hat{\omega}_{j2}(0) > 0)$, it then holds $\hat{\omega}_{j1}(t) > 0$ $(\hat{\omega}_{j2}(t) > 0)$ for all $0 \le t < \infty$. In the rest of this paper, it is assumed that $\hat{\omega}_{j1}(0) > 0$ and $\hat{\omega}_{j2}(0) > 0$.

In Fig. 1, for all $j = m, s$, $\bar{\boldsymbol{e}}_j = [\bar{e}_{j1}, \bar{e}_{j2}, \ldots, \bar{e}_{j(4n)}]^T \in \mathbb{R}^{4n}$ is defined as

$$\bar{\boldsymbol{e}}_j = \left[\boldsymbol{e}_j^T, \dot{\boldsymbol{q}}_j^T, \sqrt{\varepsilon_{j1}\hat{\omega}_{j1}}\dot{\boldsymbol{q}}_j^T, \sqrt{\hat{\omega}_{j2}}\dot{\boldsymbol{q}}_j^T\right]^T \tag{12}$$

and $\bar{\boldsymbol{e}}_{vj} = [\bar{e}_{vj1}, \bar{e}_{vj2}, \ldots, \bar{e}_{vj(4n)}]^T \in \mathbb{R}^{4n}$ is denoted by

$$\bar{\boldsymbol{e}}_{vj} = \left[\boldsymbol{e}_{vj}^T, \ddot{\boldsymbol{q}}_j^T, \frac{1}{2}\sqrt{\frac{\varepsilon_{j1}}{\hat{\omega}_{j1}}}\dot{\hat{\omega}}_{j1}\dot{\boldsymbol{q}}_j^T + \sqrt{\varepsilon_{j1}\hat{\omega}_{j1}}\ddot{\boldsymbol{q}}_j^T, \frac{1}{2}\sqrt{\frac{1}{\hat{\omega}_{j2}}}\dot{\hat{\omega}}_{j2}\dot{\boldsymbol{q}}_j^T + \sqrt{\hat{\omega}_{j2}}\ddot{\boldsymbol{q}}_j^T\right]^T. \tag{13}$$

Then, in the saturation case, by using the concept of dynamic compensation, the generalized switched filter is given as

$$\dot{\boldsymbol{y}}_j = -P_{j1}[\boldsymbol{y}_j + \boldsymbol{\mathcal{K}}_j\bar{\boldsymbol{e}}_j] - \boldsymbol{\mathcal{K}}_j\bar{\boldsymbol{e}}_{vj} + \boldsymbol{u}_j \tag{14}$$

where $\boldsymbol{y}_j = [y_{j1}, y_{j2}, \ldots, y_{j(4n)}]^T \in \mathbb{R}^{4n}$, P_{j1} is a constant positive scalar; $\boldsymbol{\mathcal{K}}_j(t) = \mathrm{diag}[\kappa_{j1}(t), \kappa_{j2}(t), \ldots, \kappa_{j(4n)}(t)] \in \mathbb{R}^{4n\times 4n}$ is the switching rule; $\boldsymbol{u}_j = [u_{j1}, \ldots, u_{j(4n)}]^T$ is defined as

$$u_{ji} = \begin{cases} -P_{j2}sgn(y_{ji} + \kappa_{ji}\bar{e}_{ji})|\dot{q}_{\ell i}(t - T_\ell)|, & 1 \le i \le n \\ 0, & i \ge n+1 \end{cases}$$

where $\dot{q}_{\ell i}(t - T_\ell)$ is the ith element of $\dot{\boldsymbol{q}}_\ell(t - T_\ell)$, P_{j2} is a positive constant scalar, $\ell = m, s$ and $\ell \neq j$. To avoid the limitation of switching frequency, the switching rule $\boldsymbol{\mathcal{K}}_j(t)$ is designed as

$$\kappa_{ji}(t) = \begin{cases} 1, \text{ if } y_{ji}(t)\bar{e}_{ji}(t) > 0 \\ \quad \text{or } y_{ji}(t)\bar{e}_{ji}(t) = 0, y_{ji}(t^-)\bar{e}_{ji}(t^-) \le 0 \\ -1, \text{ if } y_{ji}(t)\bar{e}_{ji}(t) < 0 \\ \quad \text{or } y_{ji}(t)\bar{e}_{ji}(t) = 0, y_{ji}(t^-)\bar{e}_{ji}(t^-) > 0 \end{cases} \tag{15}$$

where $i = 1, 2, \ldots, 4n$.

Remark 3.2: System (14) is a switched system with 2^{4n} modes. In fact, from the above definition, $\kappa_{ji}(t)$ $(i = 1, 2, \ldots, 4n)$ will switch between 1 and -1. Then, $\boldsymbol{\mathcal{K}}_j(t) = \mathrm{diag}[\kappa_{j1}(t), \kappa_{j2}(t), \ldots, \kappa_{j(4n)}(t)]$ has 2^{4n} possible values

$$\begin{gathered} \mathrm{diag}[-1, -1, -1, \ldots, -1] \in \mathbb{R}^{4n\times 4n} \\ \mathrm{diag}[1, -1, -1, \ldots, -1] \in \mathbb{R}^{4n\times 4n} \\ \mathrm{diag}[-1, 1, -1, \ldots, -1] \in \mathbb{R}^{4n\times 4n} \\ \vdots \\ \mathrm{diag}[-1, 1, 1, \ldots, 1] \in \mathbb{R}^{4n\times 4n} \\ \mathrm{diag}[1, 1, 1, \ldots, 1] \in \mathbb{R}^{4n\times 4n}. \end{gathered}$$

From top to bottom, number the 2^{4n} states (or called modes) in turn as: 1, 2, …, 2^{4n}. Denote the index set be $\mathcal{S}_0 = \{1, 2, \ldots, 2^{4n}\}$. Define a mapping $\bar{r}_j : \boldsymbol{\mathcal{K}}_j(t) \to \mathcal{S}_0$ as

$$\bar{r}_j(\boldsymbol{\mathcal{K}}_j(t)) = i, \text{ if and only if } \boldsymbol{\mathcal{K}}_j(t) \text{ is in the ith mode}$$

where $i \in \mathcal{S}_0$. For the sake of simplifying expression, let $r_j(t) = \bar{r}_j(\boldsymbol{\mathcal{K}}_j(t))$. Then, $r_j(t)$ can be seen as a nominal state-dependent switching signal. Further, (14) can be rewritten as the following normal switched system in a standard form

$$\dot{\boldsymbol{y}}_j(t) = \boldsymbol{\mathcal{L}}(\boldsymbol{y}_j(t), \bar{\boldsymbol{e}}_j(t), \bar{\boldsymbol{e}}_{vj}(t), \dot{\boldsymbol{q}}_\ell(t - T_\ell(t)), r_j(t)). \tag{16}$$

In what follows, let sequence $\{t_k^j\}_{k\ge 0}$ denote the switching times of $r_j(t)$. Define $\boldsymbol{s}_j(t) = \boldsymbol{y}_j(t) + \boldsymbol{\mathcal{K}}_j(t)\bar{\boldsymbol{e}}_j(t)$. Then,

$$\dot{\boldsymbol{s}}_j(t) = -P_{j1}\boldsymbol{s}_j(t) + \bar{\boldsymbol{u}}_j(t) \quad \forall t \in [t_k^j, t_{k+1}^j) \tag{17}$$

Algorithm 1: The implementation of the proposed algorithm.

Initialization (off-line):

Initialize control gains:

1: Select the appropriate K_{j1}, K_{j2}, and $\boldsymbol{K}_{j3}$;
2: Estimate $\bar{T}$ and $\tilde{T}$;
3: According to $\tilde{T}$, take P_{j2} from (20);
4: Select ϑ_j, and according to the saturation level τ_M, one can calculate P_{j1} from (20);
5: From (20), select ψ_{j11}, ψ_{j12}, ψ_{j21} and ψ_{j22};
6: Select ε_{j1} in (11);

Initialize states for $t \in [-\bar{T}, 0]$:

7: Initialize $\boldsymbol{q}_j, \dot{\boldsymbol{q}}_j = \ddot{\boldsymbol{q}}_j = \boldsymbol{0}$;
8: Compute initial errors as $\boldsymbol{e}_j = \boldsymbol{q}_j - \boldsymbol{q}_\ell$, $\boldsymbol{e}_{vj} = \dot{\boldsymbol{q}}_j - \dot{\boldsymbol{q}}_\ell$;
9: Initialize the estimators: $\hat{\omega}_{j1}, \hat{\omega}_{j2}, \dot{\hat{\omega}}_{j1} = \dot{\hat{\omega}}_{j2} = 0$;
10: Initialize $\bar{\boldsymbol{e}}_j, \bar{\boldsymbol{e}}_{vj}$;
11: Initialize the switched filter: $\boldsymbol{y}_j, \dot{\boldsymbol{y}}_j = \boldsymbol{0}$;

At sampling time $t = t_k$ **(on-line):**

1: Update the received signals from another robot, i.e., $\boldsymbol{q}_\ell(t_k - T_\ell(t_k))$ and $\dot{\boldsymbol{q}}_\ell(t_k - T_\ell(t_k))$;
2: Update tracking error $\boldsymbol{e}_j(t_k) = \boldsymbol{q}_j(t_k) - \boldsymbol{q}_\ell(t_k - T_\ell(t_k))$, and $\boldsymbol{e}_{vj}(t_k) = \dot{\boldsymbol{q}}_j(t_k) - \dot{\boldsymbol{q}}_\ell(t_k - T_\ell(t_k))$;
3: Compute the generalized control $\bar{\boldsymbol{\tau}}_j(t_k)$ from (19);
4: Compute the practical control $\boldsymbol{\tau}_j(t_k)$ from (4) and (5);
5: Substitute $\boldsymbol{\tau}_j(t_k)$ into dynamic (1), update $\ddot{\boldsymbol{q}}_j(t_k)$, $\dot{\boldsymbol{q}}_j(t_{k+1})$ and $\boldsymbol{q}_j(t_{k+1})$;
6: Update $\bar{\boldsymbol{e}}_j(t_k)$, $\bar{\boldsymbol{e}}_{vj}(t_k)$ from (12) and (13);
7: Compute switching rule $\boldsymbol{\mathcal{K}}_j(t_k)$ from (15), by using $\boldsymbol{y}_j(t_k)$ and $\bar{\boldsymbol{e}}_j(t_k)$, $\boldsymbol{y}_j(t_{k-1})$ and $\bar{\boldsymbol{e}}_j(t_{k-1})$;
8: Update $\boldsymbol{y}_j(t_{k+1})$ from (14);
9: Update adaptive estimations $\dot{\hat{\omega}}_{j1}(t_k)$, $\dot{\hat{\omega}}_{j2}(t_k)$, $\hat{\omega}_{j1}(t_{k+1})$ and $\hat{\omega}_{j2}(t_{k+1})$, from (11);

At sampling time $t = t_{k+1}$ **(on-line):**

Repeat the steps at time $t = t_k$.

where $\bar{\boldsymbol{u}}_j(t) = \boldsymbol{u}_j(t) + \boldsymbol{\mathcal{K}}_j(t)\left[\dot{T}_\ell(t)\dot{\boldsymbol{q}}_\ell^T(t - T_\ell(t)), \boldsymbol{0}_{3n}^T\right]^T$, with $\boldsymbol{0}_{3n} \in \mathbb{R}^{3n}$ denoting the $3n$-dimension zero vector. Moreover, from the definitions of $\boldsymbol{s}_j(t)$ and $\boldsymbol{\mathcal{K}}_j(t)$, it has

$$|\boldsymbol{y}_j(t)|^2 + |\bar{\boldsymbol{e}}_j(t)|^2 \le |\boldsymbol{s}_j(t)|^2 \le 2(|\boldsymbol{y}_j(t)|^2 + |\bar{\boldsymbol{e}}_j(t)|^2). \quad (18)$$

Finally, the generalized controller $\bar{\boldsymbol{\tau}}_j$ is designed as

$$\bar{\boldsymbol{\tau}}_j = -K_{j1}\dot{\boldsymbol{q}}_j - K_{j2}\boldsymbol{e}_j - \boldsymbol{K}_{j3}\boldsymbol{y}_j \quad (19)$$

which is in the form of proportional plus damping injection plus filter, where K_{j1} and K_{j2} are positive control gains; $\boldsymbol{K}_{j3} \in \mathbb{R}^{n\times 4n}$ is an appropriate nonzero matrix.

Remark 3.3: The proposed algorithm can be implemented based on Algorithm 1.

Remark 3.4: The complete controller consists of (4), (19), (14) and (11). The basic idea of the novel design is to use the concept of dynamic compensation. Specifically, if a teleoperation system becomes unstable due to the adverse effect of the actuator saturation, varying time delays, nonzero external forces, and uncertain dynamics, the $\boldsymbol{e}_j$, $\hat{\omega}_{j1}$, and $\hat{\omega}_{j2}$ and/or their derivatives will be changed. Based on the designs of (19) and (14), those changes will be first applied to the switched filter subsystem (14) and subsequently to the control torque (19). Thus, the switched filter is capable of compensating the adverse effects mentioned above. By choosing the appropriate control gains, the stability of the closed-loop system is guaranteed.

IV. Stability Analysis

To unify the study of passive and nonpassive forces, the stability is performed in the framework of SIIOS. Some notations of the stability can be found in [33], [38]. For the page limit, they are omitted here.

To perform the SIIOS, for the complete closed-loop system, denote $\boldsymbol{\chi}_j = [\boldsymbol{q}_j^T, \tilde{\omega}_{j1}, \tilde{\omega}_{j2}, \boldsymbol{y}_j^T, \bar{\boldsymbol{e}}_j^T]^T \in \mathbb{R}^{9n+2}$, $\boldsymbol{z}_j = [\tilde{\omega}_{j1}, \tilde{\omega}_{j2}, \boldsymbol{y}_j^T, \bar{\boldsymbol{e}}_j^T]^T \in \mathbb{R}^{8n+2}$. Also, let $\boldsymbol{\chi}_{jt} : [-\bar{T}, 0] \to \mathbb{R}^{9n+2}$, and $\boldsymbol{z}_{jt} : [-\bar{T}, 0] \to \mathbb{R}^{8n+2}$ denote the standard functions given by $\boldsymbol{\chi}_{jt}(\theta) = \boldsymbol{\chi}_j(t+\theta)$ and $\boldsymbol{z}_{jt}(\theta) = \boldsymbol{z}_j(t+\theta)$. By utilizing the multiple Lyapunov–Krasovskii functionals approach, then,

Theorem 4.1: The complete closed-loop master (slave) system is SIIOS with $\boldsymbol{z}_m(t)$ ($\boldsymbol{z}_s(t)$) being the output, if K_{j1}, K_{j2}, P_{j1}, P_{j2}, ψ_{j11}, ψ_{j12}, ψ_{j21}, and ψ_{j22} satisfy

$$\begin{cases} P_{j1} > \max\left\{\dfrac{(K_{j2} + \lambda_{\max}(\boldsymbol{K}_{j3}\boldsymbol{K}_{j3}^T))\tau_M}{2} + \vartheta_j, \dfrac{\tau_M}{2} + \vartheta_j, 1\right\} \\ P_{j2} \ge \tilde{T}, \ \dfrac{\psi_{j11}}{2\psi_{j12}} > \vartheta_j, \ \dfrac{\psi_{j21}}{2\psi_{j22}} > \vartheta_j \end{cases} \quad (20)$$

where $\vartheta_j > 0$ is a constant scalar, $\lambda_{max}(\boldsymbol{K}_{j3}\boldsymbol{K}_{j3}^T)$ is the largest eigenvalue of $\boldsymbol{K}_{j3}\boldsymbol{K}_{j3}^T$. Under the hypotheses, the position tracking error $\boldsymbol{e}_m(t)$ ($\boldsymbol{e}_s(t)$) will maintain bounded for any bounded exogenous force $\boldsymbol{f}_h^*$ ($\boldsymbol{f}_e^*$).

Proof: For the proof, please refer to the Appendix. ■

Remark 4.1: For the control gains in controller (19), similar to the analysis in [34], it is possible to see a tradeoff between the gains and the tracking performance. On the one hand, for fixed K_{j2}, $\boldsymbol{K}_{j3}$ and other parameters, if K_{j1} is increased, the tracking error $\boldsymbol{e}_j$ will contribute less to the control signal, which finally causes an increase in the settling time for the position tracking response; if K_{j1} is lowered, P_{j1} can only cover a smaller ϑ_j and further cause a smaller μ_j, which will result in slower convergence speed of $\boldsymbol{z}_j$. On the other hand, for any fixed K_{j1}, K_{j2}, and other parameters, if $\boldsymbol{K}_{j3}$ is increased, the output of the switched filter will contribute more to the control output, which may cause more oscillation due to the signal switching in the switched filter. Finally, it is also not suggested to take a very large K_{j2}. Because a large P_{j1} should be taken to cover the large K_{j2} at this time, while the large P_{j1} may "suspend" $\bar{\boldsymbol{e}}_j$ and $\bar{\boldsymbol{e}}_{vj}$ in switched filter (14) and then suppress the function of $\boldsymbol{K}_{j3}\boldsymbol{y}_j$ in controller (19), which may cause the undesired performance. To balance the control performance, the suggestion of the parameter selection is: K_{j1} and $\boldsymbol{K}_{j3}$ take some suitable small values, K_{j2} takes a suitable large value, while other control parameters can be selected according to Theorem 4.1.

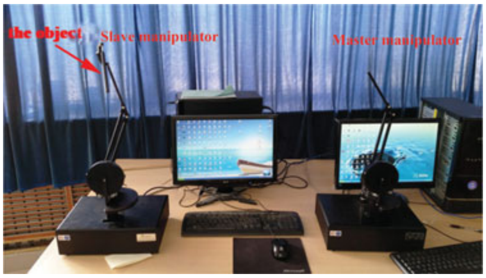

Fig. 2. Experimental teleoperation setup.

Remark 4.2: A novel adaptive control framework based on switching technique has been developed in this paper. Compared with the previous work [34], there exist both advantages and disadvantages. The main advantages lie in: 1) The external forces applied on robots by both human operator and environment can be nonpassive, while the algorithm in [34] can only handle the passive case. However, as pointed out by Polushin *et al.* [21], the passive assumption for those external forces has some strict shortcomings in practices. 2) The model parameter uncertainty has been considered, which makes the algorithm be more realistic. The main disadvantage is that the acceleration information is used in the proposed controller design, where both the master and slave robots have to equip with acceleration sensors.

Remark 4.3: On the one hand, the bounded assumption of time delay and its rate of change have been used in the derived time-dependent stability criterion, which is conservative. In future: 1) A new controller design and analysis method should be developed to handle arbitrary fast-varying time delays. 2) As discussed in Remark 2.3, some predictive control schemes, e.g., model predictive control and networked predictive control, can be developed to overcome the unity upper limit of $\dot{T}_j(t)$. On the other hand, as shown in Remark 4.2, it is also possible to account for the adaptive control without utilizing the acceleration information.

V. Experiment on a Teleoperated Pair of 3-DOF PHANToM Manipulator

The teleoperation system in the experimental setup consists of two three-DOF PHANToM Premium 1.5 A robots, which is shown in Fig. 2. (*To simulate the unknown dynamic and external disturbance, we let the slave robot grasp a rigid object that has an additional underactuated joint. On the one hand, since the rigid object has been attached to the slave robot, the slave robot's dynamic will suffer from seriously uncertainty. On the other hand, because the rigid object has an additional underactuated joint, when the slave robot tracks the master robot, the underactuated joint of rigid object will swing follow the motion of body, i.e., the slave robot, which will also introduce additional bounded disturbance.*) The two robotic manipulators are connected by two computers that communicate over a 100 Mb/s LAN. In the experimental setup, the average round-trip time delay induced by the LAN is less than 0.1ms and its standard deviation is also less than 0.1ms, which are much smaller than the 2 ms sampling period of our teleoperation. To better verify the effectiveness of the proposed control algorithm, two longer artificial communication delays that are realized by MATLAB will be introduced.

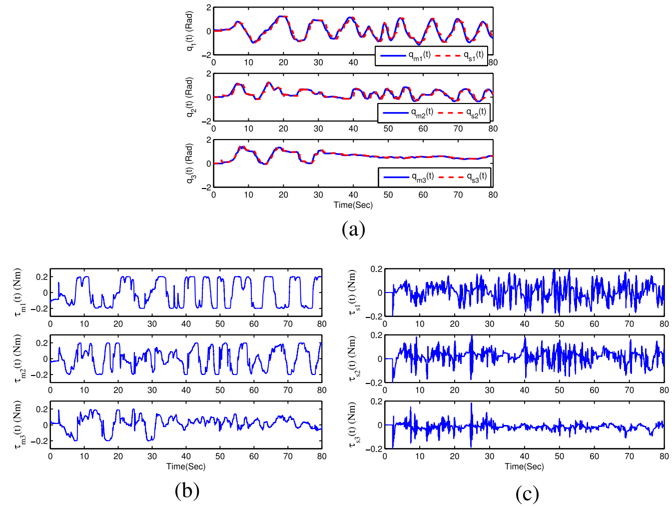

Fig. 3. Experimental results when the slave robot runs in free motion. (a) Synchronization performance. (b) Control torque τ_m. (c) Control torque τ_s.

In the experiments, the varying time delays are set to be $T_m(t) = 0.6\sin^2(t)$ and $T_s(t) = 0.4\cos^2(2t)$, which are much larger than the network time delays almost all the time. The actuator saturation for all joints of the PHANToM robot in generalized coordinate is set to be $\tau_M = 0.2$. From Theorem 4.1, the control gains are chosen as: $K_{j1} = 0.4$, $K_{j2} = 10$, $\boldsymbol{K}_{j3} = [\boldsymbol{I}_3, \boldsymbol{I}_3, \boldsymbol{I}_3, \boldsymbol{I}_3] * 0.01$, $P_{m1} = 23.7$, $P_{s1} = 22.25$, $P_{j2} = 2$, $\varepsilon_{j1} = 1$, $\psi_{j12} = \psi_{j22} = 3$, $\psi_{j11} = \psi_{j21} = 33$, with $\boldsymbol{I}_3 = diag[1, 1, 1]$, where $j = m, s$.

A. Stability Verification

The first two sets of experiments will be used to verify the stability of the proposed algorithm.

First, the slave manipulator is set to run in free motion as shown in Fig. 2. In this case, the experimental results are given in Fig. 3. Among them, Fig. 3(a) gives the joint position tracking between the master and slave robots, and obviously, the proposed nonlinear saturated control algorithm can guarantee the satisfactory tracking performance. Fig. 3(b) and (c) shows the control torques of the three joints of the master and slave robots, respectively.

The second set of experiments verifies the contact stability of the proposed algorithm. In the experiment, we put an obstacle in the first joint operation path of the slave manipulator. The tracking performance is then given as Fig. 4(a). (*Given that the master and slave robots have the same structure, only the joint positions are given here for the sake of saving space.*) From Fig. 4(a), when the slave manipulator comes in contact with the obstacle, stability is maintained and when the slave departs from the obstacle, it can track the master quickly. Finally, the control torques of the master and slave robots are shown in Fig. 4(b) and (c), respectively.

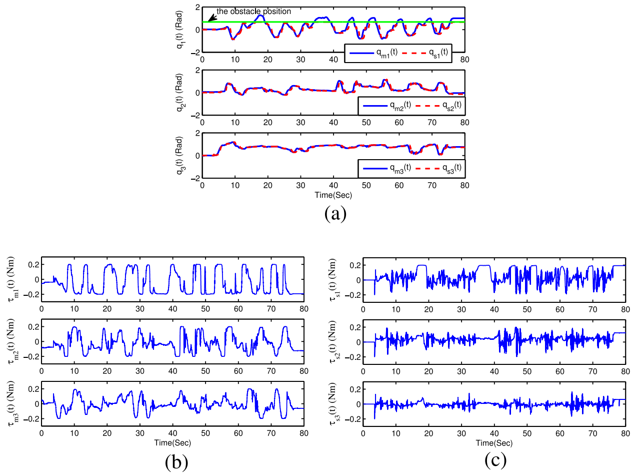

Fig. 4. Experimental results when an obstacle is located in the first joint operation path of slave robot. (a) Synchronization performance (b) Control torque τ_m (c) Control torque τ_s

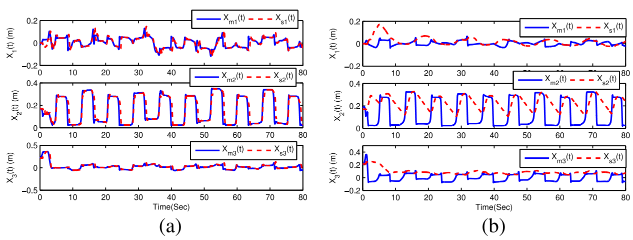

Fig. 5. Synchronization performances. (a) Synchronization performance of this paper (b) Synchronization performance of [34].

B. Comparison Study

An effective saturation control method for teleoperation system with varying time delays is investigated in [34]. This experiment verifies the adverse effect of unknown uncertainty and disturbance in robotic dynamic. The experimental setup is still given as Fig. 2. Because the slave robot has attached a rigid object that has an additional underactuated joint, its dynamic is of uncertainty, and it also suffers from unknown disturbance caused by the motion of rigid object, which have not be considered by [34].

In this experiment, to be more fair, it replaces the human operator's action in above two sets of experiments with the torque applied to master robot's motors through control. Specifically, the torque exerted on the master robot by human operator in (1), i.e., $\boldsymbol{J}_m^T(\boldsymbol{q}_m)\boldsymbol{f}_h$, is set to be $[0.22\sin(0.5t), 0.2\sin(0.35t), 0.6\sin(0.8t)]^T Nm$. Then, under the same experimental setup (including the same communication delays and the same actuator saturation, etc.), the task-space tracking performances are shown in Fig. 5. (*Although the human torque has been set to be the same, there are some differences between the motion trajectories of the master robot as shown in Figs. 5(a) and 5(b). It is mainly because the master robot is driven simultaneously by the human torque and the control torque, while the control torques generated by the control algorithms are indeed different.*) Note that, although a poor performance is observed in Fig. 5(b), the selected control

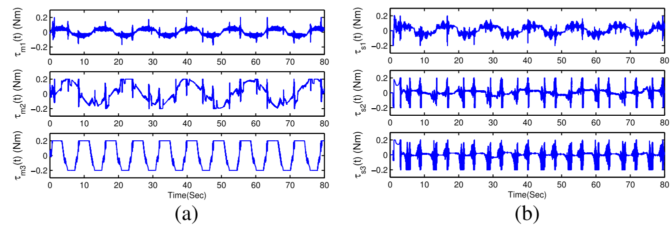

Fig. 6. Control torques under the proposed adaptive control. (a) Control torque for master robot (b) Control torque for slave robot.

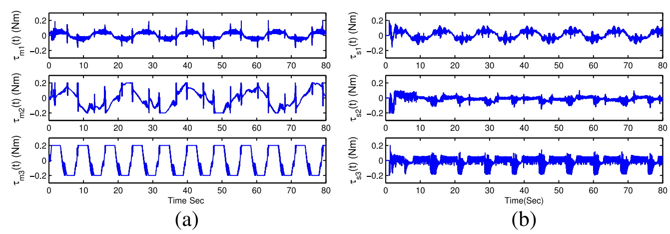

Fig. 7. Control torques under the control of [34]. (a) Control torque for master robot (b) Control torque for slave robot.

parameters for [34] in the experiment are capable to guarantee the satisfactory control performance when the rigid object is removed from the slave robot. Therefore, from Fig. 5, the control performance of [34] is adversely affected by the dynamic uncertainty and external disturbance, while in this scenario, a better performance is obtained by the proposed adaptive control algorithm of this paper.

Figs. 6 and 7 give the corresponding control torques. Although the maximum allowable torque output is set to be $\tau_M = 0.2$ for both the control of this paper and [34], the slave control torque, as shown in Fig. 7, is still less than $\tau_M = 0.2$ for most of the experiment time. Given that the performance in Fig. 5, the control of [34] does not make full use of output capacity of the actuators. In fact, in [34], it is required that $\gamma_i + N_i \leq \tau_M$, where γ_i and N_i are the upper bounds of ith element of the gravity vector $\boldsymbol{g}_j(\boldsymbol{q}_j)$ and nonlinear proportional term, respectively. It implies that the control torque should overcome the largest gravity for all time, which thus leaves less "room" for the proportional term to contribute to the control signal. Given that the gravity $\boldsymbol{g}_j(\boldsymbol{q}_j)$ is the function of $\boldsymbol{q}_j$, it does not always have the largest value. Therefore, the control of [34] is relatively conservative. In this paper, the nonlinear saturation function is placed on the outside of the generalized controller. This kind of design only requires that the $\gamma_i \leq \tau_M$, i.e., the actuators of each of the master and slave robots have the capacity to overcome the corresponding robot's gravity within their work spaces. Since the generalized controller does not consider any actuator saturation, the new design does not impose the constraint mentioned above and allows the controller to dynamically adjust the portion of the proportional control.

C. Short Remark on Control Oscillation

In Figs. 3, 4, and 6, it is found that the oscillation is fewer in the control of master robot.

First, it is mainly caused by the rigid object that has attached to the end-effector of the slave robot. On the one hand, when the slave robot tracks the master robot, the rigid object will swing follow the motion of the slave robot. If the motion of the end-effector of the slave robot is suddenly changed, the inertia of the rigid payload can generate a big drag force to the motion of the slave robot. To ensure the motion synchronization between the master and slave robots, the control torque of the slave robot should overcome the drag force, which raises more oscillations. On the other hand, the attached payload also introduces the model uncertainty, which has an adverse effect on the stability of the closed-loop slave system. In this scenario, given that the specific design of (14), the switched filter will work for the output of the control torque to ensure the stability. Since the uncertainty varies according to the motion of the slave robot, the dynamic uncertainty of slave robot is more complicated than the one in master robot. Therefore, more oscillations are found in the control torques of the slave robot.

Second, the joint speed should also be responsible for the more oscillations of the control torque of slave robot. In Figs. 3 and 4, the oscillation of joint speed is fewer in the master robot. *(On the one hand, since the master robot is manipulated by the human operator, while the human operator is capable of smoothing the joint speed, the oscillation of joint speed is reduced. On the other hand, the slave robot with an attached rigid payload has been set to run in free motion. The oscillation of joint speed cannot be reduced. In addition, due to the inertia, the attached rigid payload will also enlarge such oscillation. Therefore, the oscillation of joint speed is fewer in the master robot.)* Due to the designs of generalized controller (19) and the switched filter (14), the oscillation of $\dot{\boldsymbol{q}}_j$ will lead to the oscillation of control torque $\bar{\boldsymbol{\tau}}_j$. In fact, in the experiment of Section V-B, when we replace the human operator's action with the torque applied to master robot's motors through control, more oscillations are found in the control of the master robot.

Compared with Figs. 3(a) and 4(a), Fig. 5(a) has a more frequent change of the joint motion. Given that the design of the switched filter (14), it will cause the switching of $\boldsymbol{y}_j$. Therefore, more control oscillations are found in Fig. 6.

In practical implementation, the following measures can be taken to reduce the oscillation. On the one hand, as discussed in Remark 4.1, one can take some small $\boldsymbol{K}_{j3}$ on the premise that the stability of the closed-loop teleoperation system is ensured. On the other hand, one can also use the low-pass filter. By letting the output of the switched filter pass through a low-pass filter before it is used for the control torque, the oscillation can be reduced. More details can be found in our future work. Due to the space limit, they are omitted here.

D. Short Remark on Force Control

Force tracking is another important issue for improved transparency in bilateral teleoperation, and has attracted a lot of attention, see [9], [10], [21] and the references therein. However, most of them do not consider the actuator saturation. The existence of saturation will make the force control and its stability analysis more difficult. In this paper, the main concern is to investigate a novel adaptive control framework for teleoperation system that are subjected to actuator saturation, passive/nonpassive external forces, time-varying delays, and unknown dynamics. Similar to [34], the developed framework of this paper does not consider the force tracking control, and therefore it cannot provide the quantitative analysis of force tracking. However, due to the master controller utilizes the position error between the master and slave robots, the developed control algorithm can help the human operator feel the environment at slave site. For example, as shown in Fig. 4(a) and (b), when the first joint of the slave robot comes in contact with the obstacle, the control for the first joint of the master robot is saturated ($\tau_{m1} = -\tau_M = -0.2$). At this time, the human operator feels a large drag force, which helps the human operator understand the situation of the slave robot. Of course, the force control under actuator saturation is one of our ongoing works.

VI. Conclusion

In this paper, a novel switching-based adaptive control scheme was developed to cope with actuator saturation in nonlinear teleoperation systems that are subjected to varying time delays, dynamic uncertainty, and disturbance. To handle actuator saturation, a two-level control framework, i.e., the generalized controller plus a well-designed saturating function, was developed, while in implementation, the saturating function is placed on the outside of the generalized controller. Based on the concept of dynamic compensation, a special switched filter was investigated, and then the generalized controller was designed to be in the form as proportional plus damping injection plus switched filter. Thus, the closed-loop teleoperation system is modeled to be consisted of multiple subsystems including the robotic dynamic subsystem and the switched filter subsystem. Finally, to unify the study of passive and nonpassive external forces, the stability of the complete system was performed in the sense of SIIOS, which is established by using multiple Lyapunov–Krasovskii functionals method. For any bounded exogenous forces, it was shown that the ultimate boundedness of the position tracking errors between the master and slave robots is guaranteed.

Appendix
Proof of Theorem 4.1

The stability proof is based on [33, Lemma B.1]. For the page limit, it is omitted here. Now, let us give the proof.

Taking the Lyapunov–Krasovskii functionals

$$V_j(\boldsymbol{\chi}_{jt}, r_j(t)) = \frac{1}{2}\dot{\boldsymbol{q}}_j^T \boldsymbol{\mathcal{M}}_j \dot{\boldsymbol{q}}_j + \frac{1}{2\psi_{j12}}\tilde{\omega}_{j1}^2 + \frac{1}{2\psi_{j22}}\tilde{\omega}_{j2}^2 + \frac{1}{2}\boldsymbol{s}_j^T\boldsymbol{s}_j + \frac{\vartheta_j}{2}\int_{-\bar{T}}^{0} \boldsymbol{z}_{jt}^T(\theta)\left(\frac{-\theta}{\bar{T}} + \frac{2(\theta+\bar{T})}{\bar{T}}\right)\boldsymbol{z}_{jt}(\theta)\mathrm{d}\theta.$$

For all $r_j(t) = \mathfrak{p} \in \mathcal{S}_0$, from (18), it is easy to verify

$$\begin{cases} \bar{\rho}_{j1}|\boldsymbol{z}_j|^2 \le V_j(\boldsymbol{\chi}_{jt}, \mathfrak{p}) \le \bar{\rho}_{j2}\|\boldsymbol{z}_{jt}\|_{M_2}^2 \\ V_j(\boldsymbol{\chi}_{jt_{k+1}^j}, r_j(t_{k+1}^j)) \le V_j(\boldsymbol{\chi}_{jt_{k+1}^j}, r_j(t_k^j)),\ k \ge 0 \end{cases}$$

where $\bar{\rho}_{j1} = \min\{\frac{\rho_{j1}}{2}, \frac{1}{2\psi_{j12}}, \frac{1}{2\psi_{j22}}, \frac{1}{2}\}$, $\bar{\rho}_{j2} = \max\{\frac{\rho_{j2}}{2}, \frac{1}{2\psi_{j12}}, \frac{1}{2\psi_{j22}}, 1, \vartheta_j\}$. In addition, it also has

$$\begin{aligned} D^+V_j(\boldsymbol{\chi}_{jt}, \mathfrak{p}) &= \dot{\boldsymbol{q}}_j^T \boldsymbol{\mathcal{M}}_j \ddot{\boldsymbol{q}}_j + \frac{1}{2}\dot{\boldsymbol{q}}_j^T \dot{\boldsymbol{\mathcal{M}}}_j \dot{\boldsymbol{q}}_j + \frac{1}{\psi_{j12}}\tilde{\omega}_{j1}\dot{\tilde{\omega}}_{j1} \\ &\quad + \frac{1}{\psi_{j22}}\tilde{\omega}_{j2}\dot{\tilde{\omega}}_{j2} + \boldsymbol{s}_j^T\dot{\boldsymbol{s}}_j + \vartheta_j \boldsymbol{z}_j^T \boldsymbol{z}_j - \vartheta_j \boldsymbol{z}_{jt}^T(-\bar{T})\boldsymbol{z}_{jt}(-\bar{T}) \\ &\quad - \frac{\vartheta_j}{2\bar{T}}\int_{-\bar{T}}^0 \boldsymbol{z}_{jt}^T(\theta)\boldsymbol{z}_{jt}(\theta)\mathrm{d}\theta. \end{aligned} \tag{21}$$

On the one hand, from (6) and (19), by using Property 2.2 and Assumption 2.1, there exists $\varepsilon_{j1} > 0$ such that

$$\begin{aligned} &\dot{\boldsymbol{q}}_j^T \boldsymbol{\mathcal{M}}_j \ddot{\boldsymbol{q}}_j + \frac{1}{2}\dot{\boldsymbol{q}}_j^T \dot{\boldsymbol{\mathcal{M}}}_j \dot{\boldsymbol{q}}_j \\ &= \dot{\boldsymbol{q}}_j^T \boldsymbol{J}_j^T(\boldsymbol{q}_j)\boldsymbol{f}_{he_j} + \tau_M \dot{\boldsymbol{q}}_j^T \boldsymbol{\Xi}_j \bar{\boldsymbol{\tau}}_j - K_{he_j}\dot{\boldsymbol{q}}_j^T \boldsymbol{h}_j(\boldsymbol{q}_j) \\ &\quad - \dot{\boldsymbol{q}}_j^T \boldsymbol{f}_j(\dot{\boldsymbol{q}}_j) - \dot{\boldsymbol{q}}_j^T \boldsymbol{d}_j - \dot{\boldsymbol{q}}_j^T \boldsymbol{g}_j(\boldsymbol{q}_j) \\ &\quad - 2\dot{\boldsymbol{q}}_j^T \boldsymbol{J}_j^T(\boldsymbol{q}_j) B_{he_j} \boldsymbol{J}_j(\boldsymbol{q}_j)\dot{\boldsymbol{q}}_j \\ &\le k_6|\dot{\boldsymbol{q}}_j|^2 + \frac{1}{4}|\boldsymbol{f}_{he_j}|^2 + \tau_M \dot{\boldsymbol{q}}_j^T \boldsymbol{\Xi}_j \bar{\boldsymbol{\tau}}_j + k_1|\dot{\boldsymbol{q}}_j| + k_2|\dot{\boldsymbol{q}}_j| \\ &\quad + k_3|\dot{\boldsymbol{q}}_j|^2 + k_5|\dot{\boldsymbol{q}}_j| + k_4|\dot{\boldsymbol{q}}_j| \\ &\le \omega_{j1}|\dot{\boldsymbol{q}}_j| + \omega_{j2}|\dot{\boldsymbol{q}}_j|^2 - K_{j1}\tau_M e^{-\max_{1\le p\le n}|\bar{\tau}_{jp}|}|\dot{\boldsymbol{q}}_j|^2 \\ &\quad + \frac{K_{j2}\tau_M}{2}\dot{\boldsymbol{q}}_j^T \boldsymbol{\Xi}_j \boldsymbol{\Xi}_j \dot{\boldsymbol{q}}_j + \frac{K_{j2}\tau_M}{2}|\boldsymbol{e}_j|^2 + \frac{\tau_M}{2}|\boldsymbol{y}_j|^2 \\ &\quad + \frac{\tau_M}{2}\dot{\boldsymbol{q}}_j^T \boldsymbol{\Xi}_j \boldsymbol{K}_{j3}\boldsymbol{K}_{j3}^T \boldsymbol{\Xi}_j \dot{\boldsymbol{q}}_j + \frac{1}{4}|\boldsymbol{f}_{he_j}|^2 \\ &\le -K_{j1}\tau_M e^{-\max_{1\le p\le n}|\bar{\tau}_{jp}|}|\dot{\boldsymbol{q}}_j|^2 + \frac{1}{4}|\boldsymbol{f}_{he_j}|^2 + \frac{\tau_M}{2}|\boldsymbol{y}_j|^2 \\ &\quad + \frac{\omega_{j1}}{\varepsilon_{j1}} + \frac{K_{j2} + \lambda_{max}(\boldsymbol{K}_{j3}\boldsymbol{K}_{j3}^T)}{2}\tau_M|\dot{\boldsymbol{q}}_j|^2 \\ &\quad + \frac{K_{j2}\tau_M}{2}|\boldsymbol{e}_j|^2 + \varepsilon_{j1}\omega_{j1}|\dot{\boldsymbol{q}}_j|^2 + \omega_{j2}|\dot{\boldsymbol{q}}_j|^2. \end{aligned} \tag{22}$$

On the other hand, from (11), one can obtain

$$\begin{aligned} &\frac{1}{\psi_{j12}}\tilde{\omega}_{j1}\dot{\tilde{\omega}}_{j1} + \frac{1}{\psi_{j22}}\tilde{\omega}_{j2}\dot{\tilde{\omega}}_{j2} = -\frac{1}{\psi_{j12}}\tilde{\omega}_{j1}\dot{\hat{\omega}}_{j1} - \frac{1}{\psi_{j22}}\tilde{\omega}_{j2}\dot{\hat{\omega}}_{j2} \\ &\le -\frac{\psi_{j11}}{2\psi_{j12}}|\tilde{\omega}_{j1}|^2 - \frac{\psi_{j21}}{2\psi_{j22}}|\tilde{\omega}_{j2}|^2 - P_{j1}\varepsilon_{j1}\tilde{\omega}_{j1}|\dot{\boldsymbol{q}}_j|^2 \\ &\quad - P_{j1}\tilde{\omega}_{j2}|\dot{\boldsymbol{q}}_j|^2 + \frac{\psi_{j11}}{2\psi_{j12}}|\omega_{j1}|^2 + \frac{\psi_{j21}}{2\psi_{j22}}|\omega_{j2}|^2. \end{aligned} \tag{23}$$

Last, for any fixed $\mathfrak{p} \in \mathcal{S}_0$, from (17), one has

$$\begin{aligned} \boldsymbol{s}_j^T\dot{\boldsymbol{s}}_j &= -P_{j1}\boldsymbol{s}_j^T\boldsymbol{s}_j(t) + \boldsymbol{s}_j^T\bar{\boldsymbol{u}}_j \\ &\le -P_{j1}|\boldsymbol{y}_j|^2 - P_{j1}|\bar{\boldsymbol{e}}_j|^2 + \boldsymbol{s}_j^T\bar{\boldsymbol{u}}_j. \end{aligned}$$

For those $P_{j2} \ge \tilde{T}$, without loss of generality, it has $\boldsymbol{s}_j^T\bar{\boldsymbol{u}}_j = \sum_{i=1}^n (s_{ji}u_{ji} + s_{ji}\kappa_{ji}\dot{T}_\ell \dot{q}_{\ell i}(t - T_\ell)) \le 0$. Thus,

$$\begin{aligned} \boldsymbol{s}_j^T\dot{\boldsymbol{s}}_j &\le -P_{j1}|\boldsymbol{y}_j|^2 - P_{j1}|\boldsymbol{e}_j|^2 - P_{j1}|\dot{\boldsymbol{q}}_j|^2 \\ &\quad - P_{j1}\varepsilon_{j1}\hat{\omega}_{j1}|\dot{\boldsymbol{q}}_j|^2 - P_{j1}\hat{\omega}_{j2}|\dot{\boldsymbol{q}}_j|^2. \end{aligned} \tag{24}$$

Joining (21)–(24) with (20), one has

$$\begin{aligned} &D^+V_j(\boldsymbol{\chi}_{jt}, \mathfrak{p}) \le \vartheta_j \boldsymbol{z}_j^T\boldsymbol{z}_j - \frac{\vartheta_j}{2\bar{T}}\int_{-\bar{T}}^0 \boldsymbol{z}_{jt}^T(\theta)\boldsymbol{z}_{jt}(\theta)\mathrm{d}\theta + \frac{1}{4}|\boldsymbol{f}_{he_j}|^2 \\ &\quad - K_{j1}\tau_M e^{-\max_{1\le p\le n}|\bar{\tau}_{jp}|}|\dot{\boldsymbol{q}}_j|^2 + \frac{K_{j2}\tau_M}{2}|\boldsymbol{e}_j|^2 + \frac{\tau_M}{2}|\boldsymbol{y}_j|^2 \\ &\quad + \frac{K_{j2} + \lambda_{max}(\boldsymbol{K}_{j3}\boldsymbol{K}_{j3}^T)}{2}\tau_M|\dot{\boldsymbol{q}}_j|^2 + \frac{\omega_{j1}}{\varepsilon_{j1}} + \varepsilon_{j1}\omega_{j1}|\dot{\boldsymbol{q}}_j|^2 \\ &\quad + \omega_{j2}|\dot{\boldsymbol{q}}_j|^2 - \frac{\psi_{j11}}{2\psi_{j12}}|\tilde{\omega}_{j1}|^2 - \frac{\psi_{j21}}{2\psi_{j22}}|\tilde{\omega}_{j2}|^2 - P_{j1}\varepsilon_{j1}\tilde{\omega}_{j1}|\dot{\boldsymbol{q}}_j|^2 \\ &\quad - P_{j1}\tilde{\omega}_{j2}|\dot{\boldsymbol{q}}_j|^2 + \frac{\psi_{j11}}{2\psi_{j12}}|\omega_{j1}|^2 + \frac{\psi_{j21}}{2\psi_{j22}}|\omega_{j2}|^2 - P_{j1}|\boldsymbol{y}_j|^2 \\ &\quad - P_{j1}|\boldsymbol{e}_j|^2 - P_{j1}|\dot{\boldsymbol{q}}_j|^2 - P_{j1}\varepsilon_{j1}\hat{\omega}_{j1}|\dot{\boldsymbol{q}}_j|^2 - P_{j1}\hat{\omega}_{j2}|\dot{\boldsymbol{q}}_j|^2 \\ &\le -(P_{j1} - \vartheta_j - \frac{K_{j2} + \lambda_{max}(\boldsymbol{K}_{j3}\boldsymbol{K}_{j3}^T)}{2}\tau_M)|\dot{\boldsymbol{q}}_j|^2 \\ &\quad - (P_{j1} - \frac{K_{j2}\tau_M}{2} - \vartheta_j)|\boldsymbol{e}_j|^2 - (P_{j1} - \frac{\tau_M}{2} - \vartheta_j)|\boldsymbol{y}_j|^2 \\ &\quad - \left(\frac{\psi_{j11}}{2\psi_{j12}} - \vartheta_j\right)|\tilde{\omega}_{j1}|^2 - \left(\frac{\psi_{j21}}{2\psi_{j22}} - \vartheta_j\right)|\tilde{\omega}_{j2}|^2 \\ &\quad + \frac{1}{4}|\boldsymbol{f}_{he_j}|^2 + \frac{\omega_{j1}}{\varepsilon_{j1}} + \frac{\psi_{j11}}{2\psi_{j12}}|\omega_{j1}|^2 + \frac{\psi_{j21}}{2\psi_{j22}}|\omega_{j2}|^2 \\ &\quad - \frac{\vartheta_j}{2\bar{T}}\int_{-\bar{T}}^0 \boldsymbol{z}_{jt}^T(\theta)\boldsymbol{z}_{jt}(\theta)\mathrm{d}\theta \\ &\le -\bar{\mu}_j|\boldsymbol{z}_j|^2 - \frac{\vartheta_j}{2\bar{T}}\int_{-\bar{T}}^0 \boldsymbol{z}_{jt}^T(\theta)\boldsymbol{z}_{jt}(\theta)\mathrm{d}\theta + \Delta_j \\ &\le -\mu_j\|\boldsymbol{z}_{jt}\|_{M_2}^2 + \Delta_j \end{aligned}$$

where $\bar{\mu}_j = \min\{P_{j1} - \frac{(K_{j2}+\lambda_{max}(\boldsymbol{K}_{j3}\boldsymbol{K}_{j3}^T))\tau_M}{2} - \vartheta_j, P_{j1} - \frac{\tau_M}{2} - \vartheta_j, \frac{\psi_{j11}}{2\psi_{j12}} - \vartheta_j, \frac{\psi_{j21}}{2\psi_{j22}} - \vartheta_j\}$, $\mu_j = \min\{\bar{\mu}_j, \frac{\vartheta_j}{2\bar{T}}\}$, $\Delta_j = \frac{1}{4}|\boldsymbol{f}_{he_j}|^2 + \frac{\omega_{j1}}{\varepsilon_{j1}} + \frac{\psi_{j11}}{2\psi_{j12}}|\omega_{j1}|^2 + \frac{\psi_{j21}}{2\psi_{j22}}|\omega_{j2}|^2$.

There exists $\varepsilon_j \in (0, 1)$ such that

$$\|\boldsymbol{z}_{jt}\|_{M_2} \ge \frac{\sqrt{\Delta_j}}{\sqrt{\mu_j\varepsilon_j}} \Rightarrow D^+V_j(\boldsymbol{\chi}_{jt}, \mathfrak{p}) \le -\mu_j(1 - \varepsilon_j)\|\boldsymbol{z}_{jt}\|_{M_2}^2$$

which implies that $V_j(\boldsymbol{\chi}_{jt}, r_j(t))$ meets (36) of [33].

Following [33, Lemma B.1], it has

$$|\boldsymbol{z}_j(t)| \le \beta_j(\|\boldsymbol{z}_{j0}\|_\infty, t) + \frac{\bar{\rho}_{j2}}{\bar{\rho}_{j1}\sqrt{\mu_j\varepsilon_j}}\sqrt{\Delta_j} \tag{25}$$

where $\beta_j(\cdot, \cdot) \in \mathcal{KL}$. Hence, we complete the proof.

References

[1] P. F. Hokayem and, M. W. Spong, "Bilateral teleoperation: An historical survey," *Automatica*, vol. 42, no. 12, pp. 2035–2057, Dec. 2006.

[2] Y. Nakajima, T. Nozaki, and K. Ohnishi, "Heartbeat synchronization with haptic feedback for telesurgical robot," *IEEE Trans. Ind. Electron.*, vol. 61, no. 7, pp. 3753–3764, Jul.2014.

[3] S. Livatino *et al.* "Stereoscopic visualization and 3-D technologies in medical endoscopic teleoperation," *IEEE Trans. Ind. Electron.*, vol. 62, no. 1, pp. 525–535, Jan. 2015.

[4] W. R. Ferrell and T. B. Sheridan, "Supervisory control of remote manipulation," *IEEE Spectr.*, vol. 4, no. 10, pp. 81–88, Oct. 1967.

[5] B. Yalcin and K. Ohnishi, "Stable and transparent time-delayed teleoperation by direct acceleration waves," *IEEE Trans. Ind. Electron.*, vol. 57, no. 9, pp. 3228–3238, Sep. 2010.

[6] T. Nozaki, T. Mizoguchi, and K. Ohnishi, "Motion expression by elemental separation of haptic information," *IEEE Trans. Ind. Electron.*, vol. 61, no. 1, pp. 6192–6201, Nov. 2014.
[7] J. H. Cho, H. I. Son, D. G. Lee, T. Bhattacharjee, and D. Y. Lee, "Gain-scheduling control of teleoperation systems interacting with soft tissues," *IEEE Trans. Ind. Electron.*, vol. 60, no. 3, pp. 946–957, Mar. 2013.
[8] Y. Q. Ye, Y.-J. Pan, and T. Hilliard, "Bilateral teleoperation with time-varying delay: A communication channel passification approach," *IEEE/ASME Mechatronics*, vol. 18, no. 4, pp. 1431–1434, Aug. 2013.
[9] F. Hashemzadeh and M. Tavakoli, "Position and force tracking in nonlinear teleoperation systems under varying delays," *Robotica*, vol. 33, no. 4, pp. 1003–1016, May 2015.
[10] R. J. Anderson and M. W. Spong, "Asymptotic stability for force reflecting teleoperators with time delay," *Int. J. Robot. Res.*, vol. 11, no. 2, pp. 135–149, Apr. 1992.
[11] E. Nuño, R. Ortega, and L. Basañez, "An adaptive controller for nonlinear teleoperators," *Automatica*, vol. 46, no. 1, pp. 155–159, Jan. 2010.
[12] N. Chopra, M. W. Spong, and R. Lozano, "Synchronization of bilateral teleoperators with time delay," *Automatica*, vol. 44, no. 8, pp. 2142–2148, Aug. 2008.
[13] Y. N. Yang, C. C. Hua, and X. P. Guan, "Adaptive fuzzy finite-time coordination control for networked nonlinear bilateral teleoperation system," *IEEE Trans. Fuzzy Syst.*, vol. 22, no. 3, pp. 631–641, Jun. 2014.
[14] Y. C. Liu and M.-H. Khong, "Adaptive control for nonlinear teleoperators with uncertain kinematics and dynamics," *IEEE/ASME Mechatronics*, vol. 20, no. 5, pp. 2550–2562, Oct. 2015.
[15] H. C. Cho, J. H. Park, K. Kim, and J.-O. Park, "Sliding-mode-based impedance controller for bilateral teleoperation under varying time-delay," in *Proc. IEEE Int. Conf. Robot. Autom.*, May 2001, pp. 1025–1030.
[16] N. Chopra, P. Berestesky, and M. W. Spong, "Bilateral teleoperation over unreliable communication networks," *IEEE Trans. Control Syst. Technol.*, vol. 12, no. 2, pp. 304–313, Mar. 2008.
[17] C. C. Hua and, X. P. Liu, "Delay-dependent stability criteria of teleoperation systems with asymmetric time-varying delays," *IEEE Trans. Robot.*, vol. 26, no. 5, pp. 925–932, Oct. 2010.
[18] S. Islam, P. X. Liu, and A. E. I. Saddik, "Nonlinear control for teleoperation systems with time varying delay," *Nonlin. Dynam.*, vol. 76, no. 2, pp. 931–954, Apr. 2014.
[19] Y. Kang, Z. J. Li, X. Q. Cao, and D.-H. Zhai, "Robust control of motion/force for robotic manipulators with random time delays," *IEEE Trans. Control Syst. Technol.*, vol. 21, no. 5, pp. 1708–1718, Sep. 2013.
[20] E. Nuño, L. Basañez, and R. Ortega, "Passivity-based control for bilateral teleoperation: A tutorial," *Automatica*, vol. 47, no. 3, pp. 485–495, Mar. 2011.
[21] I. G. Polushin, S. N. Dashkovskiy, A. Takhmar, and R. V. Patel, "A small gain framework for networked cooperative force-reflecting teleoperation," *Automatica*, vol. 49, no. 2, pp. 338–348, Feb. 2013.
[22] I. G. Polushin, A. Tayebi, and H. J. Marquez, "Control schemes for stable teleoperation with communication delay based on IOS small gain theorem," *Automatica*, vol. 42, no. 6, pp. 905–915, Jun. 2006.
[23] I. G. Polushin and H. J. Marquez, "Stabilization of bilaterally controlled teleoperators with communication delay: An ISS approach," *Int. J. Control*, vol. 76, no. 8, pp. 858–870, Aug. 2003.
[24] I. Sarras, E. Nuño, and L. Basañez, "An adaptive controller for nonlinear teleoperators with variable time-delays," *J. Franklin Inst.*, vol. 351, no. 10, pp. 4817–4837, Oct. 2014.
[25] S. Islam, X. P. Liu, and A. E. Saddik, "Teleoperation systems with symmetric and unsymmetric time varying communication delay," *IEEE Trans. Instrum. Meas.*, vol. 62, no. 11, pp. 2943–2953, Nov. 2013.
[26] M. V. Kothare, P. J. Campo, M. Morari, and C. N. Nett, "A unified framework for the study of antiwindup designs," *Automatica*, vol. 30, no. 12, pp. 1869–1883, Dec. 1994.
[27] W. C. Sun, Z. L. Zhao, and H. J. Gao, "Saturated adaptive robust control for active suspension systems," *IEEE Trans. Ind. Electron.*, vol. 60, no. 9, pp. 3889–3896, Sep. 2013.
[28] H. S. Su, M. Z. Q. Chen, X. F. Wang, and J. Lam, "Semiglobal observer-based leader-following consensus with input saturation," *IEEE Trans. Ind. Electron.*, vol. 61, no. 6, pp. 2842–2850, Jun. 2014.
[29] A. Loria, R. Kelly, R. Ortega, and V. Santibáñez, "On global output feedback regulation of Euler–Lagrange systems with bounded inputs," *IEEE Trans. Automat. Control*, vol. 42, no. 8, pp. 1138–1143, Aug. 1997.
[30] E. Zergeroglu, W. Dixon, A. Behal, and D. Dawson, "Adaptive set-point control of robotic manipulators with amplitude-limited control inputs," *Robotica*, vol. 18, no. 2, pp. 171–181, Mar. 2000.
[31] S. J. Lee and H. S. Ahn, "A study on bilateral teleoperation with input saturation and systems," in *Proc. Int. Conf. Control Autom. Syst.*, Oct. 2011, pp. 161–166.
[32] S. J. Lee and H. S. Ahn, "Controller designs for bilateral teleoperation with input saturation," *Control Eng. Pract.*, vol. 33, pp. 35–47, Dec. 2014.
[33] D. H. Zhai and Y. Q. Xia, "Adaptive fuzzy control of multilateral asymmetric teleoperation for coordinated multiple mobile manipulators," *IEEE Trans. Fuzzy Syst.*, vol. 24, no. 1, pp. 57–70, Feb. 2016.
[34] F. Hashemzadeh, I. Hassanzadeh, and M. Tavakoli, "Teleoperation in the presence of varying time delays and sandwich linearity in actuators," *Automatica*, vol. 49, no. 9, pp. 2813–2821, Sep. 2013.
[35] P. Malysz and S. Sirouspour, "Nonlinear and filtered force/position mappings in bilateral teleoperation with application to enhanced stiffness discrimination," *IEEE Trans. Robot.*, vol. 25, no. 5, pp. 1134–1149, Oct. 2009.
[36] S. S. Ge, T. H. Lee, and C. J. Harris, *Adaptive Neural Network Control of Robotic Manipulators*, River Edge, NJ, USA: World Scientific, 1998.
[37] H. K. Khalil, *Nonlinear Systems*, 3rd ed., Englewood Cliffs, NJ, USA: Prentice-Hall, 2002.
[38] E. Sontag and Y. Wang, "Lyapunovcharacterizations of input to output stability," *SIAM J. Control Optim.*, vol. 39, no. 1, pp. 226–249, Jan. 2000.
[39] C. C. Hua and X. P. Liu, "Teleoperation over the internet with/without velocity signal," *IEEE Trans. Instrum. Meas.*, vol. 60, no. 1, pp. 4–13, Jan. 2011.
[40] E. Nũno, L. Basãnez, R. Ortega, and M. W. Spong, "Position tracking for non-linear teleoperators with variable time delay," *Int. J. Robot. Res.*, vol. 28, no. 7, pp. 895–910, Jul.2009.
[41] Y. Q. Xia, M. Y. Fu, and G.-P. Liu, *Analysis and Synthesis of Networked Control Systems*, Berlin, Germany: Springer, 2011.

Di-Hua Zhai was born in Anhui Province, China, in 1988. He received the B.Eng. degree in automation from Anhui University, Hefei, China, in 2010, and the M.Eng. degree in control science and engineering from the University of Science and Technology of China, Hefei, China, in 2013. He is currently working toward the Ph.D. degree at the School of Automation, Beijing Institute of Technology, Beijing, China.

His research interests include stability theory and control of teleoperation systems, switched systems, networked control systems, and stochastic systems.

Yuanqing Xia (M'15–SM'16) was born in Anhui Province, China, in 1971. He received the M.S. degree in fundamental mathematics from Anhui University, Hefei, China, in 1998, and the Ph.D. degree in control theory and control engineering from Beijing University of Aeronautics and Astronautics, Beijing, China, in 2001.

During January 2002–November 2003, he was a Postdoctoral Research Associate with the Institute of Systems Science, Academy of Mathematics and System Sciences, Chinese Academy of Sciences, Beijing, China. From November 2003 to February 2004, he was with the National University of Singapore as a Research Fellow, where he worked on variable structure control. From February 2004 to February 2006, he was with the University of Glamorgan, Pontypridd, U.K., as a Research Fellow. From February 2007 to June 2008, he was a Guest Professor with Innsbruck Medical University, Innsbruck, Austria. Since 2004, he has been with the Department of Automatic Control, Beijing Institute of Technology, Beijing, first as an Associate Professor, then, since 2008, as a Professor. His current research interests include the fields of networked control systems, robust control and signal processing, and active disturbance rejection control.